Journal of Solid State Chemistry **147,** 235–239 (1999)
Article ID jssc.1999.8245, available online at http://www.idealibrary.com on IDEAL®

Flexibility of the MPS_4^- Chains of the $KMPS_4$ (M = Ni, Pd) Compounds Studied by Molecular Orbital Calculations and Atomic Force Microscopy Measurements

M.-H. Whangbo[1]

Department of Chemistry, North Carolina State University, Raleigh, North Carolina 27695-8204

and

H. Bengel,[2] S. Jobic, and R. Brec[1]

Institut des Matériaux de Nantes, Laboratoire de Chimie des Solides, 2 rue de la Houssinière, 44322 Nantes Cedex 03, France

Received October 27, 1998; in revised form February 15, 1999; accepted February 26, 1999

The flexibility of the MPS_4^- chains of $KMPS_4$ (M = Ni, Pd) was examined by performing contact mode atomic force microscopy (AFM) measurements for the (001) surface of $KNiPS_4$ and also by performing extended Hückel tight binding calculations for the $[M(PS_4)_2]^{4-}$ entities of $KMPS_4$. The observed AFM images were analyzed by calculating the total electron density plots for an isolated $[NiPS_4]^-$ slab of the (001) surface. Our calculations show that the PS_4^{3-} ions are more strongly bound to the Pd^{2+} ions in $KPdPS_4$ than to the Ni^{2+} ions in $KNiPS_4$, and that the bonding between the PS_4^{3-} anions and M^{2+} (M = Ni, Pd) cations is flexible with respect to the rotational motions of the PS_4^{3-} anions. The AFM images recorded for the (001) surface of $KNiPS_4$ indicate that the PS_4^{3-} anions on the surface undergo a rotational relaxation when the scanning tip passes by. © 1999 Academic Press

1. INTRODUCTION

The structures of the compounds $KMPS_4$ (M = Ni, Pd) (1, 2) contain the MPS_4^- chains made up of PS_4^{3-} tetrahedra and M^{2+} (d^8) cations (Fig. 1a). Every M^{2+} ion is located at the center of a square planar unit MS_4 sharing edges with two adjacent PS_4^{3-} tetrahedra, so that adjacent MS_4 units are perpendicular to each other. These chains form layers of MPS_4^- chains parallel to the *ab*-plane as shown in Figs. 1b and 1c. The chain direction of Fig. 1b is perpendicular to that of Fig. 1c. These two kinds of layers alternate along the *c*-axis direction, and the K^+ ions reside between the layers at the sites made up of eight S atoms.

When the $KMPS_4$ compounds are dissolved in a polar organic solvent such as dimethylformamide (DMF), the MPS_4^- chains become flexible polymer chains (3, 4). In the DMF solution of $KNiPS_4$, fragmentation and rearrangement take place to form trimer units $[(NiPS_4)_3]^{3-}$. However, in the DMF solution of $KPdPS_4$, this phenomenon does not occur and the $PdPS_4^-$ chains are maintained at room temperature (3, 4). As demonstrated by force valence field calculations (4), these observations imply that the PS_4^{3-} anions are more strongly bound to the Pd^{2-} cations than to the Ni^{2+} cations. Moreover, the chemical and physical properties of the MSP_4^- chains in solution indicate that the bending and rotational motions of the PS_4^{3-} anions in a MPS_4^- chain (Figs. 2a and 2b, respectively) do not require much energy.

The above implications can be easily verified by performing molecular orbital calculations for the $[M(PS_4)_2]^{4-}$ unit that is formed between the M^{2+} and two PS_4^{3-} ions. However, it is desirable to find another piece of experimental evidence supporting the flexibility of bonding between the M^{2+} and the two PS_4^{3-} ions. Scanning tunneling and atomic force microscopy (AFM) have shown (5, 6) that during imaging, nonequivalent atoms of surface undergo different degrees of local structure relaxation under the repulsive forces the tip exerts to the surface. The tip-force induced surface relaxation can modify the local electronic structure of a surface (7) and can even bring about a reversible rearrangement of weak metal–metal bonds (8). As shown in Fig. 1, the (001) surface of $KMPS_4$ consists of parallel MPS_4^- chains in which the square planar MS_4 units are either perpendicular or parallel to the surface. Thus, when the (001) surface of $KMPS_4$ is examined by AFM, the scanning tip might induce the rotation of the PS_4^{3-} anions

[1]To whom correspondence should be addressed.
[2]Present address: MICRONAS INTERMETALL Gmbh, Hans-Bunte-Strasse 19, D-79108 Freiburg, Germany.

0022-4596/99 $30.00

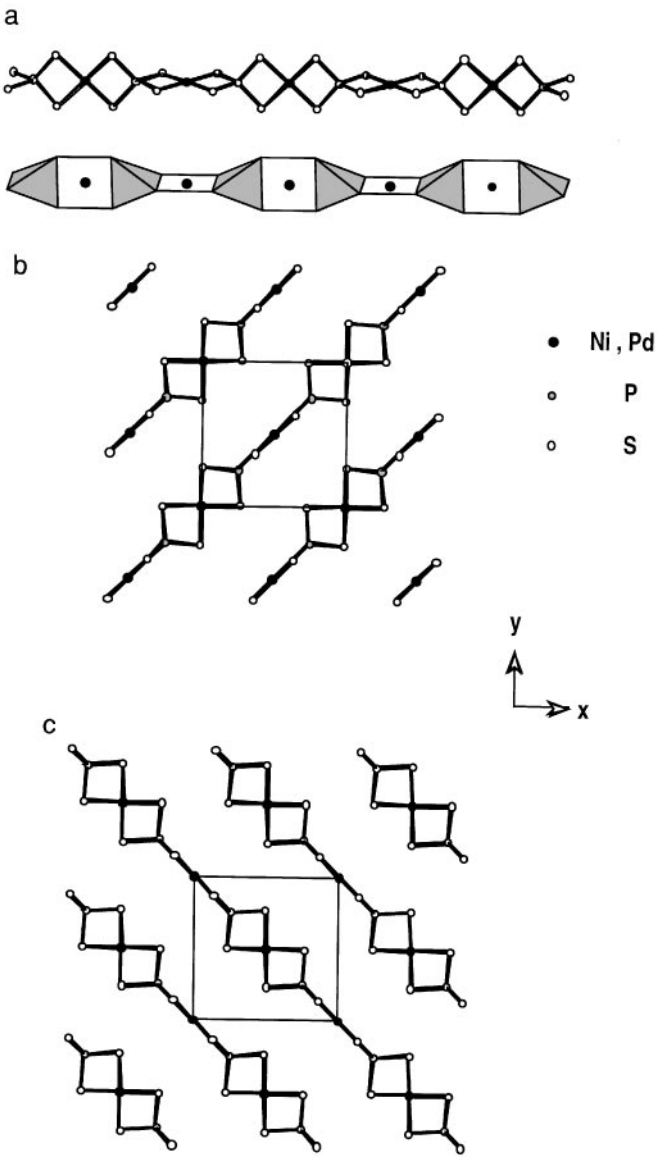

FIG. 1. Structure building blocks of KMPS$_4$: (a) Two perspective views of a MPS$_4^-$ chain. In the lower representation, each PS$_4^{3-}$ anion is represented by a shaded tetrahedron. (b, c) Projection views of two adjacent layers of MPS$_4^-$ chains, where the square boxes represent a unit cell.

on the surface if the rotational motion of the PS$_4^{3-}$ anions (Fig. 2b) does not require much energy as suggested by the dissolution studies (3, 4). Thus, AFM images of KMPS$_4$ may differ substantially than those expected for the ideal (001) surface taken from the bulk crystal structure. In the present work, we examine the flexibility of the MPS$_4^-$ chains in the solid state by studying the (001) surface of KNiPS$_4$ with AFM and also by performing molecular orbital calculations for the $[M(PS_4)_2]^{4-}$ unit (M = Ni, Pd) using the extended Hückel tight-binding (EHTB) method (9, 10).

2. BINDING ENERGIES AND ROTATIONAL POTENTIALS

The $[M(PS_4)_2]^{4-}$ (M = Ni, Pd) unit is made up of the M^{2+} (d^8) cation and two PS$_4^{3-}$ anions. Thus, the binding energy ΔE of the $[M(PS_4)_2]^{4-}$ unit can be estimated from the energy of the $[M(PS_4)_2]^{4-}$ unit by subtracting the energy of the M^{2+} cation and two PS$_4^{3-}$ anions. Calculations of the ΔE values show that the M^{2+} and PS$_4^{3-}$ ions are more strongly bound in $[Pd(PS_4)_2]^{4-}$ than in $[Ni(PS_4)_2]^{4-}$ by 63 kJ/mol. This is consistent with the experimental observation that a fragmentation–rearrangement process takes place in the DMF solution of KNiPS$_4$, but not in the DMF solution of KPdPS$_4$ (3, 4). Figure 3 shows the rotational potential energy curves calculated for $[M(PS_4)_2]^{4-}$ as a function of the rotational angle ϕ defined in Fig. 2b. The potential is soft for both $[Pd(PS_4)_2]^{4-}$ and $[Ni(PS_4)_2]^{4-}$. For example, at $\phi = 40^\circ$, the potential energy increases are only 20 and 26 kJ/mol for $[Ni(PS_4)_2]^{4-}$ and $[Pd(PS_4)_2]^{4-}$, respectively. Thus, the PS$_4^{3-}$ anions of the $M(PS_4)^-$ chains can easily rotate away from the square planar MS_4 arrangements.

3. CHARACTERIZATION OF THE (001) SURFACE BY AFM

Contact-mode AFM measurements were made on freshly cleaved surfaces of the mounted crystal samples of KNiPS$_4$ at ambient conditions using a commercial scanning probe microscope Nanoscope III (Digital Instruments, Inc.) and

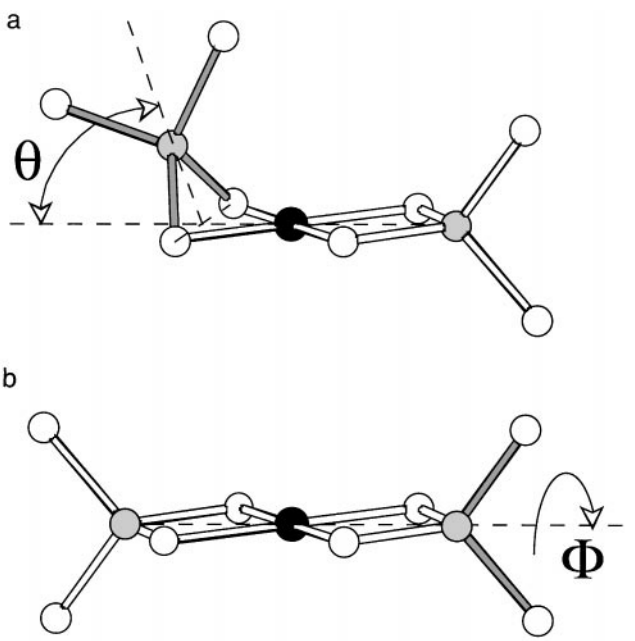

FIG. 2. (a) Bending and (b) rotational motions of one PS$_4^{3-}$ anion in the $[M(PS_4)_2]^{4-}$ unit.

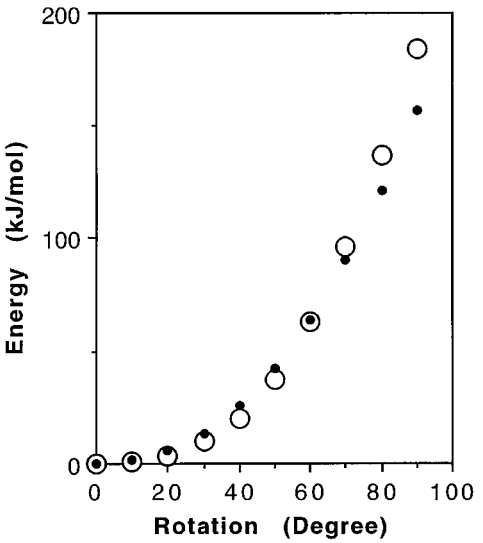

FIG. 3. Rotational potential energy curves calculated for the $[M(PS_4)_2]^{4-}$ unit as a function of the rotational angle ϕ. The large empty and small filled circles represent M = Ni and M = Pd, respectively.

commercial cantilevers with Si_3N_4 tips. Atomic-scale images were recorded in the height imaging mode. To observe image contrast, it was necessary to use a weak cantilever with long and thin arms as well as low set-point forces (about 20 nN). Use of higher forces resulted in a poor image quality or even the loss of any image contrast. Images corresponding to the surface slab of K^+ cations were not observed, and this is due most probably to the mechanical instability of such a layer.

AFM images of a surface are well described by the total electron density plot $\rho(r_0)$ calculated for the surface (5). To simulate the $\rho(r_0)$ plot for the (001) surface of $KNiPS_4$, we use a single layer of $NiPS_4^-$ chains taken from the bulk crystal structure of $KNiPS_4$. The $\rho(r_0)$ plots were calculated using the EHTB method (9–11) with the tip placed at 0.5 Å above the highest-lying atoms of the sample surface (i.e., $r_0 = 0.5$ Å). The essential features of these plots do not depend on r_0.

Figure 4a shows the $\rho(r_0)$ plot calculated for a single layer of $NiPS_4^-$ chains taken from the bulk crystal structure of $KNiPS_4$. In this layer, the arrangements of the PS_4^{3-} anions were kept as in the bulk crystal structure of $KNiPS_4$ (see Fig. 1b). The surface represented by this layer is an unrelaxed one and will be referred to as the $(0°, 0°)$-structure (see below). As expected from the topography of this unrelaxed surface, the high electron density (HED) spots of the $\rho(r_0)$ plot correspond to the highest-lying S atom of each PS_4^{3-} anion. Thus, if no surface relaxation takes place during AFM measurements, there should be two equally bright spots per unit cell in the AFM images recorded for the (001) surface of $KNiPS_4$. However, the observed AFM images differ from this picture, as will be discussed below.

Figure 5a shows a representative AFM image recorded for the (001) surface of $KNiPS_4$. To emphasize the periodic features of this image, a zoomed part of this image was filtered using the fast Fourier transform procedure as presented in Fig. 5b. This image shows one bright and three less bright spots per unit cell. The distance between the brightest spots are 9.1 Å, which compare well with the corresponding value (i.e., 8.2538 Å) determined from the crystal structure within the typical experimental error of 10% in AFM measurements. The distances from the brightest to the less bright spots are about 4.1 and 3.6 Å from the image, which correspond to 3.7 and 3.2 Å, respectively, when scaled down by the factor of 8.3/9.1. The distance of 3.7 Å is comparable in length to the longest S ⋯ S distance (3.548 Å) found within a PS_4^{3-} anion. Likewise, the distance of 3.2 Å is comparable in length to the shortest S ⋯ S distance (3.177 Å) between two adjacent PS_4^{3-} anions (i.e., one S ⋯ S side of the NiS_4 square).

To explain why the observed AFM images of $KNiPS_4$ exhibit more than two bright spots per unit cell, we suppose that the PS_4^{3-} anions undergo a rotational motion around the chain axis in order to reduce the tip-sample repulsive interaction associated with the higher-lying sulfur atoms. When a PS_4^{3-} anion undergoes a rotation from the unrelaxed structure, the highest-lying S atom is lowered in height. At the same time, the rotation raises the height of one of the two S atoms lying in the NiS_4 plane parallel to the

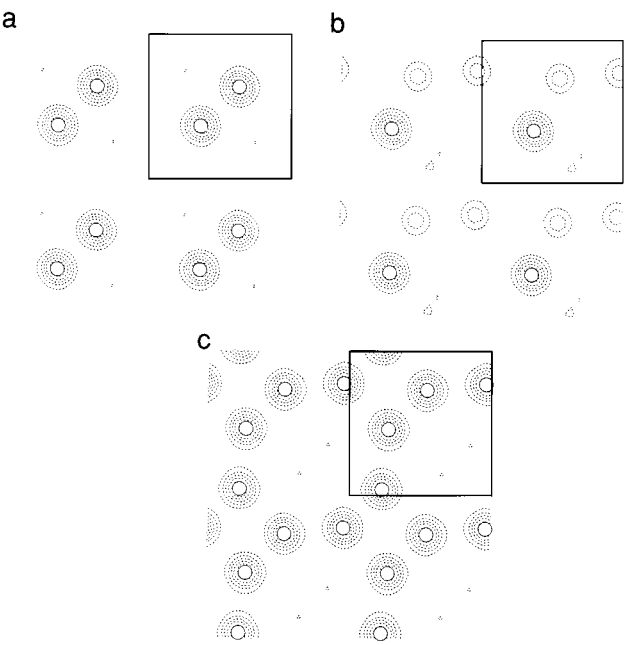

FIG. 4. $\rho(r_0)$ plots calculated for the (001) surface of $KNiPS_4$. The plots in (a), (b), and (c) refer to the $(0°, 0°)$-, $(0°, 45°)$-, and $(45°, 45°)$-structures, respectively (see the text). The values of the contour lines are 0.04, 0.07, 0.11, 0.15, and 0.19 electrons/au^3, and the circles represent the highest-lying S atoms.

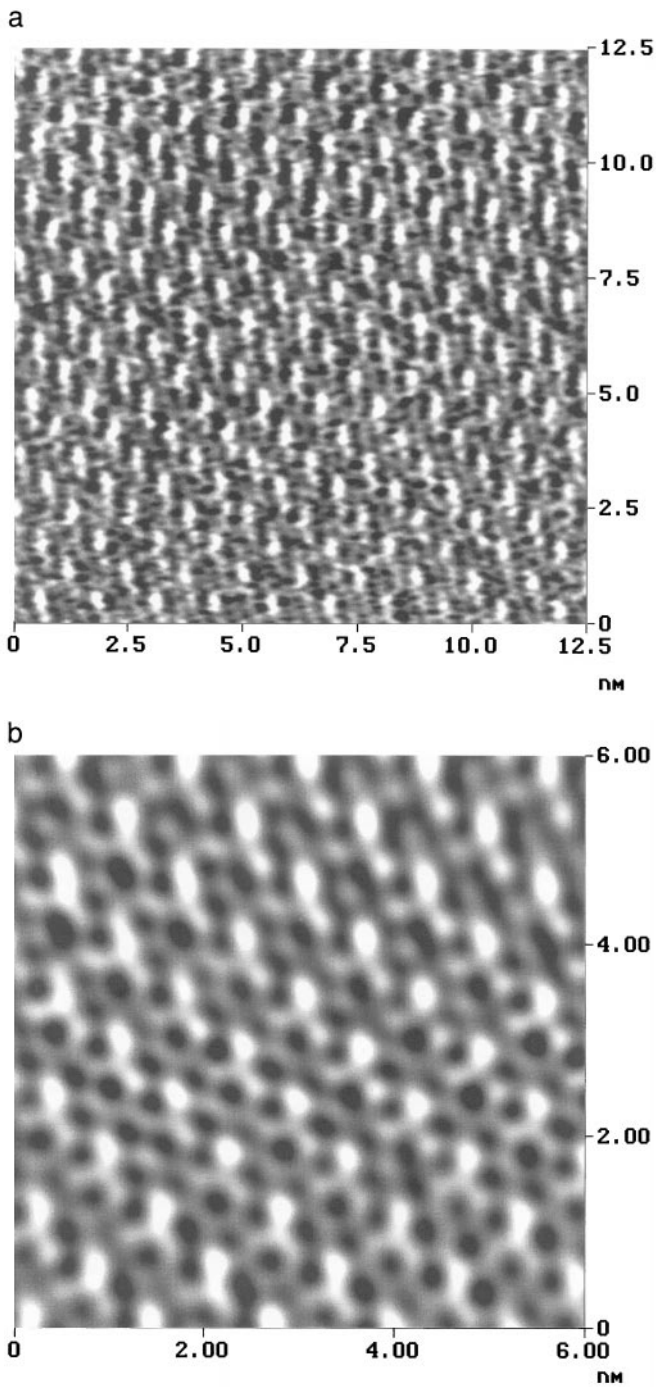

FIG. 5. Representative AFM height images recorded for the (001) surface of $KNiPS_4$ with the scan rate of 20.35 Hz. (a) Unfiltered image. (b) Filtered image. The contrast variation covers from 0.0 to 1.0 nm.

(001) surface (see Fig. 1a). When a PS_4^{3-} anion is rotated by 45°, its highest-lying two S atoms have the same height. For simplicity, we will consider two extreme cases of the PS_4^{3-} anion rotation. In one case every second PS_4^{3-} anion of each $NiPS_4^-$ chain is rotated by 45°, and the resulting layer of $NiPS_4^-$ chains will be referred to as the $(0°, 45°)$-structure. In the other case, every PS_4^{3-} anion of each $NiPS_4^-$ chain is rotated by 45°, and the resulting layer of $NiPS_4^-$ chains will be referred to as the $(45°, 45°)$-structure, in which the Ni atoms remain in square-planar environments. Figures 4b and 4c show the $\rho(r_0)$ plots calculated for the $(0°, 45°)$- and the $(45°, 45°)$-structures, respectively. These plots show that depending on the extent of the rotation, each PS_4^{3-} anion can contribute two HED spots.

When the angle of rotation is less than 45°, two complications arise. First, the two highest-lying S atoms of PS_4^{3-} are unequal in heights so that their HED spots will have unequal densities. Second, the lateral positions of these unequal HED spots depend on the sense of the rotational direction (e.g., $+30°$ vs $-30°$). AFM measurements involve a large tip-sample contact area (5), and the sense and the magnitude of rotation may not be the same for all the PS_4^{3-} anions in the tip-sample contact area. Therefore, the observed AFM images should represent an average of all these complex contributions. Our assumption that the PS_4^{3-} ions on the (001) surface undergo a rotational relaxation provides a natural explanation for why the observed AFM image shows more than two bright spots per unit cell.

4. CONCLUDING REMARKS

Our calculations show that the PS_4^{3-} ions are more strongly bound to the Pd^{2+} ions in $KPdPS_4$ than to the Ni^{2+} ions $KNiPS_4$, in support of the observation of the dissolution studies (3, 4). Furthermore, our calculations show soft potential curves for the rotation of the PS_4^{3-} anions around the MPS_4^- chain axis. Thus, during AFM imaging, the PS_4^{3-} anions are expected to undergo a rotational relaxation to reduce the tip-sample repulsive interaction associated with the higher-lying sulfur atoms. In agreement with this expectation, the AFM images recorded for the (001) surface of $KNiPS_4$ exhibit a brightness pattern different than the one expected for the unreconstructed (001) surface. This provides a strong support for the observation of the dissolution studies (3, 4) that the MPS_4^- chains of the compounds $KMPS_4$ (M = Ni, Pd) are flexible.

ACKNOWLEDGMENTS

The work at North Carolina State University was supported by the Office of Basic Energy Sciences, Division of Materials Sciences, U.S. Department of Energy, under Grant DE-FG05-86ER45259. H. B. thanks la Région des Pays de la Loire for the financial support (Grant 185757F) during his stay at the Institut des Matériaux de Nantes.

REFERENCES

1. S. H. Elder, A. Van der Lee, R. Brec, and E. Canadell, *J. Solid State Chem.* **116,** 107 (1995).
2. K. Chondroudis, M. Kanatzidis, J. Sayettat, S. Jobic, and R. Brec, *Inorg. Chem.* **36,** 5859 (1997).

3. J. Sayettat, L. M. Bull, J.-C. P. Gabriel, S. Jobic, F. Camerel, A.-M. Marie, M. Fourmigé, P. Batail, R. Brec, and R.-L. Ingelbert, *Angew. Chem. Int. Ed.* **37,** 1711 (1998).
4. J. Sayettat, L. M. Bull, S. Jobic, J.-C. P. Gabriel, M. Fourmigé, P. Batail, R. Brec, R.-L. Ingelbert, and C. Sourisseau, *J. Mat. Chem.* **9,** 143 (1999).
5. S. N. Magonov, M.-H. Whangbo, "Surface Analysis with STM and AFM," VCH, Weinheim, 1996.
6. H. Bengel, H.-J. Cantow, M. Evain, S. N. Magonov, and M.-H. Whangbo, *Surf. Sci.* **365,** 461 (1996).
7. S. N. Magonov, H.-J. Cantow, and M.-H. Whangbo, *Surf. Sci. Lett.* **318,** L1175 (1994).
8. H. Bengel, H.-J. Cantow, S. N. Magonov, and M.-H. Whangbo, *Adv. Mater.* **7,** 5 (1995).
9. R. Hoffmann, *J. Chem. Phys.* **39,** 1397 (1963).
10. M.-H. Whangbo and R. Hoffmann, *J. Am. Chem. Soc.* **100,** 6093 (1978).
11. Our EHTB calculations were performed using the CAESAR package (J. Ren, W. Liang and M.-H. Whangbo, *Crystal and Electronic Structure Analysis Using CAESAR*, *1998*, http://www.primec.com). The atomic parameters of Ni, P, and S atoms were taken from Ref. (1), and those of Pd are as follows: The H_{ii} values are -12.02 eV for 4*d*, -7.32 eV for 5*s*, and -3.75 eV for 5*p*. The exponents of the Slater type orbitals (STO's) are 2.190 for 5*s*, and 2.152 for 5*p*. The 4*d* orbital is represented as a linear combination of two STO's of exponents 5.983 and 2.613 with coefficients 0.5264 and 0.6373, respectively. For the calculation of the off-diagonal elements H_{ij}, the weighted formula was used [J. Ammeter, H.-B. Bürgi, J. Thibeault, and R. Hoffmann, *J. Am. Chem. Soc.* **100,** 3686 (1978)].